



HAL
open science

Theoretical and experimental study of heat transfer through a vertical partitioned enclosure: application to the optimization of the thermal resistance

V. Sambou, B. Lartigue, F. Monchoux, M. Adj

► To cite this version:

V. Sambou, B. Lartigue, F. Monchoux, M. Adj. Theoretical and experimental study of heat transfer through a vertical partitioned enclosure: application to the optimization of the thermal resistance. Applied Thermal Engineering, 2008, 28 (5-6), pp.488. 10.1016/j.applthermaleng.2007.05.008 . hal-00498955

HAL Id: hal-00498955

<https://hal.science/hal-00498955>

Submitted on 9 Jul 2010

HAL is a multi-disciplinary open access archive for the deposit and dissemination of scientific research documents, whether they are published or not. The documents may come from teaching and research institutions in France or abroad, or from public or private research centers.

L'archive ouverte pluridisciplinaire **HAL**, est destinée au dépôt et à la diffusion de documents scientifiques de niveau recherche, publiés ou non, émanant des établissements d'enseignement et de recherche français ou étrangers, des laboratoires publics ou privés.

Accepted Manuscript

Theoretical and experimental study of heat transfer through a vertical partitioned enclosure: application to the optimization of the thermal resistance

V. Sambou, B. Lartigue, F. Monchoux, M. Adj

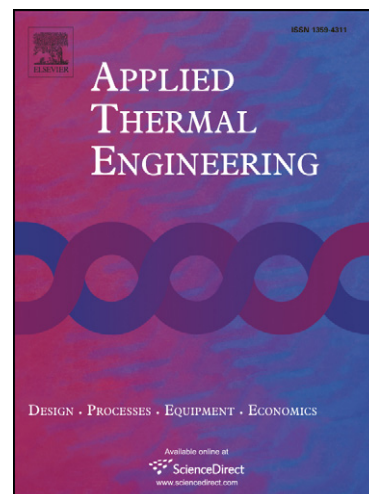
PII: S1359-4311(07)00186-X
DOI: [10.1016/j.applthermaleng.2007.05.008](https://doi.org/10.1016/j.applthermaleng.2007.05.008)
Reference: ATE 2175

To appear in: *Applied Thermal Engineering*

Received Date: 28 June 2006
Revised Date: 11 May 2007
Accepted Date: 12 May 2007

Please cite this article as: V. Sambou, B. Lartigue, F. Monchoux, M. Adj, Theoretical and experimental study of heat transfer through a vertical partitioned enclosure: application to the optimization of the thermal resistance, *Applied Thermal Engineering* (2007), doi: [10.1016/j.applthermaleng.2007.05.008](https://doi.org/10.1016/j.applthermaleng.2007.05.008)

This is a PDF file of an unedited manuscript that has been accepted for publication. As a service to our customers we are providing this early version of the manuscript. The manuscript will undergo copyediting, typesetting, and review of the resulting proof before it is published in its final form. Please note that during the production process errors may be discovered which could affect the content, and all legal disclaimers that apply to the journal pertain.



Theoretical and experimental study of heat transfer through a vertical partitioned enclosure: application to the optimization of the thermal resistance

V. Sambou^{a,b}, B. Lartigue^{*a}, F. Monchoux^a, M. Adj^b

^a*P.H.A.S.E., Université Paul Sabatier, 118 route de Narbonne, 31062 Toulouse Cedex 9, France*

^b*L.E.A., Ecole Supérieure Polytechnique, BP 5085 Dakar Fann, Sénégal*

Abstract

Enclosures divided by multiple vertical diffusive partitions have high insulating qualities and may provide tangible benefits as a construction material. In this study, we have developed one-dimensional analytical model of coupled heat transfer (conduction, convection, radiation) in such enclosures. This model is numerically and experimentally validated for an important number of configurations and size of alveolus. The variation of the thermal resistance versus the number of partitions has been experimentally validated. The model is then used to find the partitions number that maximizes the thermal resistance of a partitioned enclosure. Effects of thermal and geometrical parameters on the maximal thermal resistance of the partitioned enclosure have been also investigated. We have shown that the thermal resistance could be improved by decreasing the thermal conductivity of walls; decreasing the emissivity of the partitions faces; or using very thin partitions. The use of relatively thick exterior vertical walls marginally degrades the optimal thermal resistance while at the same time increases the thermal inertia. The combination of the different parameters gives a set of solutions when one desires to obtain precise characteristics for an insulating envelope. The presented model can help to determine the most suitable combination of parameters allowing to get the desired maximal thermal resistance.

Keywords: partitioned enclosure; heat transfer; thermal resistance; optimization

* lartigue@cict.fr

Tel: +33.5.61.55.69.94 ; fax: +33.5.61.55.81.54

1. Introduction

Residential and commercial buildings represent 46% of the total energy consumption in France [1], becoming the first final energy consuming. Corresponding greenhouse gas emission represents a quarter of the total emission. The Kyoto protocol aims reduce energy consumption and greenhouse gas emissions in residential as well as commercial buildings. As a consequence, in its thermal standards, the building code recommends industrial development of products with strengthened thermal insulation for opaque building walls [2]. Yet, high insulation which decreases heating energy during winter period leads to overheating during hot days. To overcome this phenomenon using thermal inertia is an efficient way [3]. Construction materials with non-localized insulation aim to have this double property: they both are insulating materials and have a high heat capacity that increases thermal inertia of the building. Among these materials, alveolar materials have an important place.

Enclosures with vertical partitions may describe such construction material [4]. They have been efficiently used to reduce conduction, convection and radiation heat transfer. In addition to alveolar materials, other engineering applications recover from such a system, like alveolar solar collectors, cryogenic storage, etc.

Laminar natural convection in differentially heated rectangular cavities has been studied extensively [5, 6]. More recently, several works outline the decrease of heat transfer using partitioned enclosures. Andersen and Bejan reported in [7] the decrease of the overall heat transfer in single and double partitioned enclosure, both theoretically and experimentally. Other studies focus on the only natural convection heat transfer in enclosures divided by one [8, 9] or multiple [10] non-diffusive partitions, showing that partitioned enclosures compare favorably with fully insulating the enclosure with a porous material [8]. The coupled conduction-convection heat transfer is studied when considering thick partitions by Ho and Yih [11] in a single partitioned enclosure as well as by Kangni et al.[12] and Turkoglu and Yücel [13] in multiple partitioned enclosures. These studies mainly emphasize the decrease of heat transfer by reducing the size of the alveolus. Radiation heat

transfer is rarely taken into account although it is as important as the convection heat transfer. The complexity of three-dimensional coupled heat transfer as well as the complexity of the geometry of alveolar materials make difficult to optimize these products.

In this study, we have established an analytical model of conduction-convection-radiation heat transfer for an enclosure with multiple vertical diffusive partitions, representing more closely real applications. The performances of the system calculated with the analytical model have been compared with both the results of a numerical model and experimental results. The validated analytical model is then used to evaluate the sensitivity of geometrical parameters and thermal properties to the thermal resistance.

2. Heat transfer through partitioned enclosures

2.1 Geometry

The studied system is a two-dimensional partitioned enclosure of internal height H , internal width L and a supposed infinite depth (Fig. 1). The four external walls of the enclosure have a thickness e_w . N partitions of thickness e_p are equally placed in the enclosure. The enclosure has therefore $(N+1)$ alveolus of thickness e_a calculated by:

$$e_a = \frac{L - Ne_p}{N + 1} \quad (1)$$

2.2 One-dimensional analytical heat transfer model

Constant uniform temperatures T_H and T_C are imposed at external surfaces of vertical walls. Heat transfer is supposed one-dimensional in the enclosure. The enclosure is segmented into three visible parts on Fig. 1. The heat transfer is evaluated for a unit length in the Oy direction.

2.2.1 Heat transfer through horizontal walls (parts 1 and 3)

In parts 1 and 3 the thermal conduction resistance is calculated using:

$$R_1 = R_3 = \frac{T_h - T_c}{Q_w} = \frac{L + 2e_w}{k_w e_w} \quad (2)$$

where k_w is the thermal conductivity of the walls.

2.2.2 Heat transfer through the alveolus (part 2)

In the part 2, heat flow calculation should be computed taking into account either conduction or convection occurring in the alveolus, as well as radiation between the alveolus faces. T_{h_i} and T_{c_i} are hot and cold faces temperatures of the alveolus i , respectively.

■ If heat flux through the alveolus occurs by conduction, calculation is performed with:

$$Q_{cd_i} = k_a H \frac{T_{h_i} - T_{c_i}}{e_a} \quad (3)$$

■ If the heat flux is convective, it is then given by:

$$Q_{cv_i} = k_a Nu_i H \frac{T_{h_i} - T_{c_i}}{e_a} \quad (4)$$

The Nusselt number in the alveolus i (Nu_i) is given by Bejan correlation [6]:

$$Nu_i = 0.364 Ra_i^{1/4} A_i^{-1} \quad (5)$$

where Ra_i is the Rayleigh number and A_i the aspect ratio of the alveolus i .

$$Ra_i = \beta_i g \frac{(T_{h_i} - T_{c_i})}{\alpha_i \nu_i} H^3 \quad \text{and} \quad A_i = \frac{H}{e_a} \quad (6)$$

where β_i is the thermal expansion coefficient; α_i the air thermal diffusivity and ν_i the air kinematic

viscosity calculated at $T_{m_i} = \frac{T_{h_i} + T_{c_i}}{2}$.

■ Calculation of the radiation heat transfer in the cavities supposes that air is a non-participant media, and that the radiative exchange of horizontal faces is negligible. Vertical faces are assumed to be perfectly diffuse with a constant emissivity coefficient. Then, radiation flux between cold and hot faces of the alveolus i is given by:

$$Q_{rad_i} = h_{rad_i} H (T_{h_i} - T_{c_i}) \quad (7)$$

The radiative coefficient h_{rad_i} is given by [14]:

$$h_{\text{rad}_i} = \frac{1}{\left(\frac{1-\varepsilon_{h_i}}{\varepsilon_{h_i}} + \frac{1-\varepsilon_{c_i}}{\varepsilon_{c_i}} + \frac{1}{F_{hc}} \right)} 4\sigma T_{m_i}^3 \quad (8)$$

where ε_{h_i} and ε_{c_i} are the emissivity coefficients of hot and cold faces of alveolus i , respectively;

F_{hc} is the view factor; T_{m_i} is the mean temperature in the alveolus i .

■ The global heat flux through the alveolus i is therefore given by:

$$Q_{g_i} = h_{g_i} H (T_{h_i} - T_{c_i}) \quad (9)$$

$$\text{with } h_{g_i} = \frac{\max(k_a; k_a Nu_i)}{e_a} + h_{r_i} \quad (10)$$

Heat flux through the left and right external vertical walls of the envelope is given respectively by:

$$Q_{w_1} = k_w H \frac{(T_h - T_{h_1})}{e_w} \quad \text{and} \quad Q_{w_2} = k_w H \frac{(T_{c_{(N+1)}} - T_c)}{e_w} \quad (11)$$

Similarly, the flux through a partition j is given by:

$$Q_{p_j} = k_p H \frac{(T_{c_j} - T_{h_{(j+1)}})}{e_p} \quad (12)$$

Finally, using the conservation of the flux in steady state, the total flux can be calculated from the temperature difference $(T_h - T_c)$ by:

$$Q_{\text{tot}} = H \frac{(T_h - T_c)}{\left(2 \frac{e_w}{k_w} + N \frac{e_p}{k_p} + \sum_{i=1}^{N+1} \frac{1}{h_{g_i}} \right)} \quad (13)$$

T_{h_i} , T_{c_i} and Q_{tot} computation is made by solving iteratively equations (10) to (13). Thermal

resistance of the part 2 is then given by:

$$R_2 = \frac{(T_h - T_c)}{Q_{\text{tot}}} = \frac{\left(2 \frac{e_w}{k_w} + N \frac{e_p}{k_p} + \sum_{i=1}^{N+1} \frac{1}{h_{g_i}} \right)}{H} \quad (14)$$

2.2.3 Total resistance of the whole partitioned enclosure

The total resistance of the whole enclosure is determined with the thermal resistances R_1 , R_2 and R_3 in parallel. The total resistance for a unit of surface (r_{tot}) is therefore given by:

$$r_{tot} = (H + 2e_w) \frac{R_1 R_2 R_3}{R_1 R_2 + R_1 R_3 + R_2 R_3} \quad (15)$$

2.3 Two-dimensional numerical heat transfer model in partitioned enclosure

■ Actually, as soon as the convection takes place in alveolus, heat transfer is two-dimensional. The proposed numerical model consists in computing Navier-Stokes and energy equations. Using the Boussinesq approximation to account for density variation (in vertical direction), the steady state laminar non-dimensional continuity and momentum equations can be written as:

$$\frac{\partial U}{\partial X} + \frac{\partial W}{\partial Z} = 0 \quad (16)$$

$$\begin{cases} U \frac{\partial U}{\partial X} + W \frac{\partial U}{\partial Z} = -\frac{\partial P}{\partial X} + \left(\frac{Pr}{Ra}\right)^{\frac{1}{2}} \left(\frac{\partial^2 U}{\partial X^2} + \frac{\partial^2 U}{\partial Z^2}\right) \\ U \frac{\partial W}{\partial X} + W \frac{\partial W}{\partial Z} = -\frac{\partial P}{\partial Z} + \left(\frac{Pr}{Ra}\right)^{\frac{1}{2}} \left(\frac{\partial^2 W}{\partial X^2} + \frac{\partial^2 W}{\partial Z^2}\right) + \theta \end{cases} \quad (17)$$

$$U \frac{\partial \theta}{\partial X} + W \frac{\partial \theta}{\partial Z} = (Ra Pr)^{-\frac{1}{2}} \left(\frac{\partial^2 \theta}{\partial X^2} + \frac{\partial^2 \theta}{\partial Z^2}\right) \quad (18)$$

where U and W are the dimensionless velocity components in the x and z direction, respectively. P and θ are the dimensionless pressure and temperature. Dimensionless parameters are defined as:

$$X = \frac{x}{H}; Z = \frac{z}{H}; U = \frac{u}{W_0}; W = \frac{w}{W_0} \text{ with } W_0 = \sqrt{g\beta_0(T_h - T_c)H}$$

$$P = \frac{p}{\rho W_0^2}; \theta = \frac{T - T_0}{T_h - T_c} \text{ with } T_0 = \frac{T_h + T_c}{2}$$

Pr is the Prandtl number defined as $Pr = \frac{\nu_a}{\alpha_a}$

■ Radiation between alveolus faces is calculated using the discrete ordinates method. Air in the alveolus is supposed semi-transparent non-diffusing medium with very small absorption coefficient.

Alveolus faces are assumed to be opaque and perfectly diffuse for the infrared radiation. The radiative flux leaving the surface of an alveolus face is given by:

$$q_{\text{rad}} = (1-\varepsilon)q_{\text{in}} + \varepsilon\sigma T_s^4 \quad (19)$$

where the incident radiative heat flux q_{in} can be given by solving the radiative transfer equation (RTE) [15].

■ In solid parts the two-dimensional steady state heat transfer is governed by:

$$\frac{\partial^2 \theta}{\partial X^2} + \frac{\partial^2 \theta}{\partial Z^2} = 0 \quad (20)$$

with the following boundary conditions:

$$\theta(0, Z) = \frac{1}{2} ; \theta\left(\frac{L}{H}, Z\right) = -\frac{1}{2} ; \frac{\partial \theta}{\partial Z}\bigg|_{Z=0} = 0 ; \frac{\partial \theta}{\partial Z}\bigg|_{Z=1+\frac{2e_w}{H}} = 0 \quad (21)$$

A uniform, tight (401 x 603) (X,Z) grid - ensuring independence of the solution on the grid size - is used. The set of equations was computed using the computational fluid dynamics software Fluent [16], based on the finite volumes method. In order to compare the results with those of the analytical model, the mean temperature is calculated at alveolus faces by:

$$\theta_m(X) = \int_{\frac{e_w}{H}}^{1+\frac{e_w}{H}} \theta(X, Z) dZ \quad (22)$$

Average Nusselt number in an alveolus is calculated from:

$$Nu_{cv} = \frac{\frac{1}{H} \int_{\frac{e_w}{H}}^{e_w+H} q_{cv}(z) dz}{q_{\text{ref}}} \quad (23)$$

where q_{ref} is the average conduction heat transfer in the case where convection does not develop.

$q_{cv}(y)$ is the local parietal flux, calculated as:

$$q_{cv}(z) = k_a(z) \frac{(T_i(z) - T_i(z))}{\Delta x} \quad (24)$$

where $T_i(z)$ is the temperature of the face i and $T_i(z)$ is the temperature of the very close node in the viscous air layer.

Similarly, radiative Nusselt number is defined by:

$$\text{Nu}_{\text{rad}} = \frac{\frac{1}{H} \int_{e_w}^{e_w+H} q_{\text{rad}}(z) dz}{q_{\text{ref}}} \quad (25)$$

where $q_{\text{rad}}(y)$ is the local radiation flux at the alveolus face.

In order to validate the numerical code, one reproduces in Table 1 results of Wang et al. [17] for an air-filled square cavity differentially heated in which natural convection is coupled with radiation. Results of other authors [18] on a same square cavity in which only convection is studied are also reported. The agreement is good: the maximal deviation with [17] in Nusselt number is 1%.

2.4 Experimental study

A PVC partitioned enclosure has been built (Fig. 2a). Internal dimensions of the enclosure are $H=0.184$ m, $L=0.285$ m and 0.275 m of depth. External walls have a thickness $e_w=0.008$ m. 1 to 47 vertical partitions of thickness $e_p=0.003$ m are placed between the vertical walls of the enclosure, creating therefore different configurations from 2 to 48 equal width alveolus. Thermal properties of the solid parts are the thermal conductivity of the PVC [2] ($k_w = k_p = 0.17 \text{ W}\cdot\text{m}^{-1}\cdot\text{K}^{-1}$) and the faces emissivity ($\epsilon=0.9$). Physical air properties are $\beta_i = 3.49 \cdot 10^{-3} \text{ K}^{-1}$, $\alpha_a = 1.96 \cdot 10^{-5} \text{ m}^2\cdot\text{s}^{-1}$, $\nu_a = 1.46 \cdot 10^{-5} \text{ m}^2\cdot\text{s}^{-1}$.

When it is possible, thermocouples (type K) are placed on each partition at points A, B, C and D as indicated on Fig. 2b. Points of measures A to C permit to highlight the temperature stratification on Oz direction. Measures on points B and D are used to check the two-dimension of the problem. The thermocouples are standardized and the temperature uncertainty is estimated to 0.3K. Heat transfer through the partitioned enclosure is experienced in a calibrated hot-box (Fig. 3). Two highly insulated chambers are clamped tightly together to surround the test enclosure. The cold and hot chambers are metering and thermally controlled. Two fluxmeters ($100 \times 100 \text{ mm}^2$) are placed on the hot and cold sides of the enclosure. The fluxmeter precision given by the constructor is 5%. The climatic chamber is the one used for U-value measurements of a whole wall according to the standard ISO 8990 [19]. The apparatus has been modified for the characterization of a single brick

[20].

Temperatures and parietal flux are regularly measured with a datalogger driven by a computer until the steady state is reached. The experimental thermal resistance of the partitioned enclosure is determined by:

$$r_{\text{exp}} = \frac{T_{\text{h_exp}} - T_{\text{c_exp}}}{q_{\text{exp}}} \quad (26)$$

where $T_{\text{h_exp}}$ is the average hot face temperature, $T_{\text{c_exp}}$ is the average cold face temperature and q_{exp} the average parietal flux measured on the hot face and on the cold face.

Table 2 reports the problem parameters of the seven configurations of the partitioned enclosure experimentally studied, i.e. the partitions number N , the aspect ratio A of a cavity and the temperature difference ($T_{\text{h}}-T_{\text{c}}$) of the whole enclosure. The temperature difference values are imposed by the experiments. These configurations have been chosen to characterize different modes of heat transfer, as can be shown on Fig. 4. Indeed, according to Yin et al. [21] and Batchelor [22], pure conduction occurs in the cavities of configurations A to D while established convection regime is expected for configurations F and G. Configuration E is in the transition zone.

3. Validation of the analytical model

Although all the 7 configurations of the enclosure have been numerically and experimentally studied, only results of configurations G ($N=3$, $T_{\text{h}}-T_{\text{c}}=23.2$ K) and D ($N=11$, $T_{\text{h}}-T_{\text{c}}=29.7$ K) are presented in detail, since they are characteristic of two different flow regimes (Fig. 4) in air-filled cavities.

3.1 Numerical validation

Tables 3 and 4 report convective and radiative analytical Nusselt numbers. In the enclosure G, $Nu_{\text{cv}} \gg 1$ (Table 3) in all alveolus indicates that convection develops. Radiative flux represents 2/3 of the total heat transfer. In the enclosure D, convection is slight with $Nu_{\text{cv}} \cong 1$ (Table 4). Radiative flux is still higher than the convective one. These results show the predominance of radiative flux over

convection in alveolus. This is due to the high emissivity of the material (PVC) used here and to the low local Rayleigh number in cavities (about $1.9 \cdot 10^5$ for case G and $2.3 \cdot 10^3$ for case D). Therefore one can not study this type of enclosure without taking into account the radiation [23].

The analytical model allows to compare contributions of radiation and convection. If temperature difference in cavities is low, i.e. T_h close to T_c or N high (configurations A to D), convection does not occur. Only conduction heat transfer occurs in air cavities. Radiation and the conduction heat transfer vary simultaneously with the temperature difference in cavities and the ratio between them remains more or less constant. Moreover, if the temperature difference in cavities increases sufficiently - it occurs theoretically when $(T_h - T_c)$ reaches a limit value and/or when N is low (configurations F and G) - convection takes place in cavities. The convection heat flux increases more rapidly than the radiative one until the two modes balance.

In Fig. 5 numerical isotherms contours are plotted for configurations G and D, respectively. In addition to the expected two-dimensional flow, these patterns also confirm the complete establishment of the convection in the enclosure G contrarily to the enclosure D, in accordance with the prediction of the diagram on Fig. 4.

Tables 5 and 6 present radiative and convective numerical Nusselt numbers in the alveolus of the enclosures G and D, respectively. The numerical values of Nu_{rad} are very closed to the analytical ones. The maximal difference is 1.3%. On the other hand, the numerical values of convection Nusselt numbers are lower than those obtained analytically. The maximal difference is 25% for enclosure G and 18% for enclosure D. This maximal difference takes place in the first and last cavities for the two cases. The analytical model overestimates the convection heat flux in cavities. It is due to the fact that Bejan correlation used here is established for cavities with isotherm faces. When convection decreases, the temperature stratification decreases on the faces of cavities and the difference between Nu_{cv} given by the two models decreases and tends to zero when convection stops.

Analytical, numerical and experimental dimensionless mean temperatures at alveolus faces are plotted in Fig. 6. These graphs show a great agreement between analytical and numerical

temperatures. Indeed, the maximal difference between analytical and numerical temperatures is about 0.1K for both enclosures G and D.

Except the values of Nu_{cv} presenting a non negligible difference when convection develops, the numerical results match the analytical ones; this is a first validation of the analytical model.

3.2 Experimental validation

Fig. 6 compares also analytical and experimental dimensionless temperatures at alveolus faces. These graphs show a good agreement between analytical and experimental results. The maximal difference between analytical and mean experimental temperatures is 0.6K for enclosure G and 0.9K for enclosure D. Although these maximal values are higher to the uncertainty of the thermocouples estimated to 0.3K, the results shown here can be considered as another validation of the analytical model.

Fig. 7 presents dimensionless temperatures at points A, B and C placed on a vertical line on partitions for the partitioned enclosure G and D. These graphs show measured temperature stratification on alveolus faces, confirming the two-dimension of the temperature field. The maximal temperature difference between points A and C is 2.9 K for enclosure G and 2.5 K for enclosure D. The mean value of this difference is 2 K for enclosure G and 1.5 K for enclosure D. These values confirm that convection is more established in enclosure G than in enclosure D.

In order to determine the importance of the three-dimension of the problem, Fig. 8 presents dimensionless experimental temperatures at points B and D placed on a horizontal line on partitions for the partitioned enclosures G and D. These temperatures are practically the same. Indeed, the maximal temperature difference between points B and D is 0.3 K for enclosure G and 0.9 K for enclosure D. For enclosure D, only two values of the temperature difference between points B and D are superior to the thermocouple uncertainty. These values are erroneous. These results show that the third dimension according y does not intervene in the heat transfer in the enclosure even with a small partitions number. This remark justifies limiting the numerical study to two-dimensional model.

3.3 Comments

The analysis of numerical and experimental results allows us to use with confidence the analytical model presented in 2.2, to describe heat transfer through the partitioned enclosure.

Indeed, this analytical model is a simplified expression of the two-dimensional modeling of the thermal transfer in enclosures. Radiation heat transfer calculation takes into account the geometry of the alveolus through the view factor F_{ij} . The aspect ratio is sufficiently high to neglect the horizontal side effects. The two-dimensional aspect of the convection heat transfer is taken into account with the aspect ratio in Bejan relation [6]. The radiation has the effect to attenuate temperature stratification on faces and then justifies the validity of the use of Bejan relation. In the case of conduction heat transfer – preponderant when convection does not occur – only the presence of horizontal walls causes the two-dimensionality of heat transfer. The thickness of these walls is very low in relation to the height of the cavity; therefore, the heat flux through these horizontal walls is very small in comparison with the one through the partitioned enclosure.

The model is therefore validated, regardless of the number of partitions placed in the enclosure. A later validation will be performed with the determination of the number of partitions that maximizes the thermal resistance of the material.

4. Application: optimization of the thermal resistance

4.1 Maximal thermal resistance

Thermal resistance through alveolar material as described above varies with the number of partitions. Indeed, the increase of the number of partitions reduces radiative and convective flux in alveolus. On the other hand, this increase furthers conduction in the solid parts of the enclosure. Therefore limiting heat transfer through the material implies to find the optimal partitions number leading to the maximal thermal resistance. This calculation is made theoretically using the analytical model of the partitioned enclosure that has been validated. Experimental determination is made by measuring the thermal resistance of the enclosure in configuration A to G.

Fig. 9 shows the variation of the thermal resistance versus the number of partitions. Bars of

experimental resistance uncertainty are added in the graph. This curve shows a good agreement between theory and experiments. The existence of a maximum indicates that there is an optimal number of partitions that induces a maximal thermal resistance.

The maximal thermal resistance achieves a compromise between two phenomena: the conduction and the radiation heat transfer. Indeed, the more the number of partitions, the more conduction heat flux since the partitions are more conductive than air. Thus, the conduction thermal resistance decreases when N increases. On the other hand, the addition of a partition causes a reduction of the temperature difference in cavities and therefore the radiation heat transfer decreases. Then the radiation thermal resistance increases with N . The thermal resistance being the sum of two values varying in an opposite way with N , it exists an optimal number of partitions for which this resistance is maximal.

This number of partitions is equal to 45 in our case (PVC enclosure). The optimal number of partitions obtained with the analytical model is constant if the temperature difference ($T_h - T_c$) varies over a constant mean temperature value; it increases slowly with the mean temperature. The optimal number varies with different parameters as shown in following.

4.2 Case of a construction material: influence of parameters

The validated analytical model has been then used to determine the thermal resistance of an enclosure made with a construction material. A parametric study for the partitioned enclosure has been made according to the thermal conductivity of the material of the enclosure (Fig. 10a), the emissivity of alveolus faces (Fig. 10b), the thickness of partitions (Fig. 10c) and the vertical wall thickness of the enclosure (Fig. 10d). The geometry of the enclosure is the same described in Fig. 1. The considered parameter only varies.

4.2.1 Thermal conductivity of the partitioned enclosure

Fig. 10a illustrates the influence of thermal conductivity of the material of the partitioned enclosure on the optimal number of partitions. The graphs outline two phenomena. First, the optimal number

of partitions slightly decreases to a limiting value when the thermal conductivity increases. The limiting value is 40 partitions corresponding to an alveolus thickness of about 0.004 m for our case. Material thermal conductivity has a small influence on the optimal number of partitions (from 40 to 43 in Fig. 10a), but of course a great one on the thermal resistance which increases (from 1.2 to 3.6 $\text{m}^2 \cdot \text{K} \cdot \text{W}^{-1}$) when thermal conductivity decreases. Secondly, when k is high, the variation of the thermal resistance presents a tray around the optimal value. Indeed, as soon as the convection stops in cavities, the reduction of radiation by addition of a partition has the same order of magnitude than the increase of conduction flux. Therefore, the total heat flux varies slowly. For instance, for the case of $k = 2.2 \text{ W} \cdot \text{m}^{-1} \cdot \text{K}^{-1}$, the optimal number could be reduced of half without the thermal resistance is modified.

4.2.2 Walls and partitions emissivity

In order to model a classic brick, material is considered to be terra cotta ($k=1.04 \text{ W} \cdot \text{m}^{-1} \cdot \text{K}^{-1}$). Fig. 10b shows that the diminution of the alveolus faces emissivity improves the optimal thermal resistance of the enclosure. This result is predicable due to the fact that radiation represents the highest part of heat transfer in alveolus. It is worth noting that the optimal number of partitions decreases quasi linearly with the emissivity. The emissivity variation from 0.9 to 0.1 decreases the optimal number of partitions from 40 to 16 corresponding to an increase of the alveolus thickness from 0.004 m to 0.014 m. The aspect ratio A decreases from a value of 46 to 13.2. The diminution of the partitions number can constitute an economy on the material used for the manufacture.

4.2.3 Thickness of partitions

Considered material is still terra cotta. The partitions thickness has a strong influence on the thermal resistance of the enclosure when the partitions number is high (Fig. 10c). This influence is weak when the partitions number is low because the quantity of material is small in this case. The optimal resistance decreases when the partitions thickness increases. This result is predicable because by increasing the partitions thickness one increases the contribution of conduction in the

solid parts into the total heat transfer through the whole enclosure. The use of thin partition improves the thermal resistance. For example, using partitions of 0.001 m of thickness instead of 0.003 m partitions increases the optimal resistance of about 20%.

4.2.4 Thickness of vertical external walls

Fig. 10d shows that the increase of the thickness of external vertical walls of the partitioned enclosure has a modest influence on the resistance. Indeed, the use of vertical walls of 0.020 m of thickness instead of 0.008 m reduces the maximal thermal resistance only about 4%. This result is important because it shows that one can improve the thermal inertia of the partitioned enclosure by increasing only the vertical wall thickness without degrading very significantly the thermal resistance.

5. Conclusion

A one-dimensional analytical electrical analogy model-based can be used to evaluate correctly thermal performances such as the thermal resistance of partitioned enclosures where heat transfer is two-dimensional. Prominent role of the radiative transfer in partitioned enclosures, which is commonly neglected, has been established. The analytical model validated by experiments is used to determine the number of equally distributed partitions that minimizes heat transfer. We have shown that the thermal resistance of the partitioned enclosure could be improved by decreasing the thermal conductivity of the partitions; decreasing the emissivity of walls; or by using very thin partitions. Finally, the use of relatively thick external vertical walls marginally degrades the maximal thermal resistance while at the same time increases the thermal inertia.

The combination of the different parameters gives a set of solutions when one desires to obtain precise characteristics for an insulating envelope. The space is sufficiently large to overcome economic and technical constraints that accompany the elaboration of a product. The presented model can help to determine the most suitable combination of parameters allowing to get the desired maximal thermal resistance.

Nomenclature

A	alveolus aspect ratio
e	thickness (m)
g	acceleration due to gravity ($\text{m}\cdot\text{s}^{-2}$)
H	height (m)
h	convective coefficient ($\text{W}\cdot\text{m}^{-2}\cdot\text{K}^{-1}$)
k	thermal conductivity ($\text{W}\cdot\text{m}^{-1}\cdot\text{K}^{-1}$)
L	width (m)
N	partition number
Nu	Nusselt number $\left(\text{Nu} = \frac{q \cdot e_a}{k_a} \right)$
P	dimensionless pressure
Pr	Prandtl number
Q	flux (W)
q	heat flux density ($\text{W}\cdot\text{m}^{-2}$)
R	Thermal resistance ($\text{K}\cdot\text{W}^{-1}$)
r	surfacic thermal resistance ($\text{m}^2\cdot\text{K}\cdot\text{W}^{-1}$)
Ra	Rayleigh number
T	temperature (K)
u, v, w	velocity components ($\text{m}\cdot\text{s}^{-1}$)
U, V, W	dimensionless velocity components
x, y, z	Cartesian coordinates (m)
X, Y, Z	dimensionless Cartesian coordinates

Greek letters

α	thermal diffusivity ($\text{m}^2\cdot\text{s}^{-1}$)
β	thermal expansion coefficient (K^{-1})
ε	emissivity
ν	kinematic viscosity ($\text{m}^2\cdot\text{s}^{-1}$)
θ	dimensionless temperature
σ	Stefan Boltzmann Constant

Subscripts

a	air
h	hot
cv	convective
c	cold
exp	experimental
g	global
in	incident
m	mean
p	partition
rad	radiative
ref	reference
s	surface
tot	total
w	wall

References

- [1] <http://www.iea.org/>
- [2] Guide RT 2000, Réglementation thermique 2000, CSTB, France (2004).
- [3] K.A. Antonopoulos, E.P. Koronaki. On the dynamic thermal behaviour of indoor spaces. *Applied Thermal Engineering*, 21 (9) (2001) 929-940.
- [4] B. Lacarrière, B. Lartigue, F. Monchoux, Numerical study of heat transfer in a wall of vertically perforated bricks: influence of assembly method, *Energy and Buildings* 35 (3) (2003) 229-237.
- [5] I. Catton, Natural convection in enclosures, in: *Proceedings of the 6th International Heat Transfer Conference*, Toronto, Vol. 6, 1978, pp. 13-43.
- [6] A. Bejan, *Convection Heat Transfer*, 2nd ed., Wiley, New York, 1995
- [7] R. Anderson, A. Bejan, Heat transfer through single and double vertical walls in natural convection: theory and experiment, *International Journal of Heat and Mass Transfer* 24 (10) (1981) 1611-1620.
- [8] T. W. Tong, F. M. Gerner, Natural convection in partitioned air-filled rectangular enclosures, *International Communications in Heat and Mass Transfer* 13 (1986) 99-108.
- [9] T. Nishimura, M. Shiraishi, Y. Kawamura, Natural convection heat transfer in enclosures with an off-center partition, *International Journal of Heat and Mass Transfer* 30 (8) (1987) 1756-1758.
- [10] T. Nishimura, M. Shiraishi, F. Nagasawa, Y. Kawamura, Natural convection heat transfer in enclosures with multiple vertical partitions, *International Journal of Heat and Mass Transfer* 31 (8) (1988) 1679-1686.
- [11] C.J. Ho, Y.L. Yih, Conjugate natural convection heat transfer in an air-filled rectangular cavity, *International Communications in Heat and Mass Transfer* 14 (1987) 91-100.
- [12] A. Kangni, R. Ben Yedder, E. Bilgen, Natural convection and conduction in enclosures with multiple vertical partitions, *International Journal of Heat and Mass Transfer* 34 (11) (1991) 2819-2825.
- [13] H. Turkoglu, N. Yücel, Natural convection heat transfer in enclosures with conducting multiple partitions and side walls, *Heat and Mass Transfer* 32 (1996) 1-8.
- [14] J-F. Saccadura, *Initiation aux transferts thermiques*, Tech. & Doc., Lavoisier, 1993

- [15] G. Colomer, M. Costa, R. Consul, A. Oliva, Three-dimensional numerical simulation of convection and radiation in a differentially heated cavity using the discrete ordinates method, *International Journal of Heat and Mass Transfer* 47 (2004) 257-269.
- [16] Fluent, Fluent 6.1, User's guide, Fluent Inc., 2003.
- [17] Hong Wang, Shihe Xin, Patrick Le Quéré, Étude numérique du couplage de la convection naturelle avec le rayonnement de surfaces en cavité carrée remplie d'air, *Comptes Rendus Mécanique* 334 (2006) 48–57.
- [18] A. Abdelbaki et Z. Zrikem, 1999, Simulation numérique des transferts thermiques couplés à travers les parois alvéolaires des bâtiments. *International Journal of Thermal Science* 38 (1999) 719-730.
- [19] ISO 8990, Thermal Insulation-Determination of Steady –State Thermal Transmission Properties-Calibrated and Guarded Hot Box, International Standard Organization, 1996.
- [20] B. Laccarière, A. Trombe, F. Monchoux, Experimental unsteady characterization of heat transfer in a multi-layer wall including air layers – Application to vertically perforated bricks, *Energy and Building* 38 (3) (2006) 232-237.
- [21] S.H. Yin, T.Y. Wung, K. Chen, Natural convection in an air layer enclosed within rectangular cavities, *International Journal of Heat and Mass Transfer* 21 (1978) 307-315.
- [22] G.K. Batchelor, Heat transfer by free convection across a closed cavity between vertical boundaries at different temperatures, *Quarterly of Applied Mathematics* 12 (1954) 209-233.
- [23] X. Nicolas, G. Lauriat, J. Jimenez Rondan, Etude numérique des transferts de chaleur couplés dans une paroi alvéolaire, Congrès Français de Thermique, SFT 2005, Reims, 30 mai – 2 juin 2005.

Figures

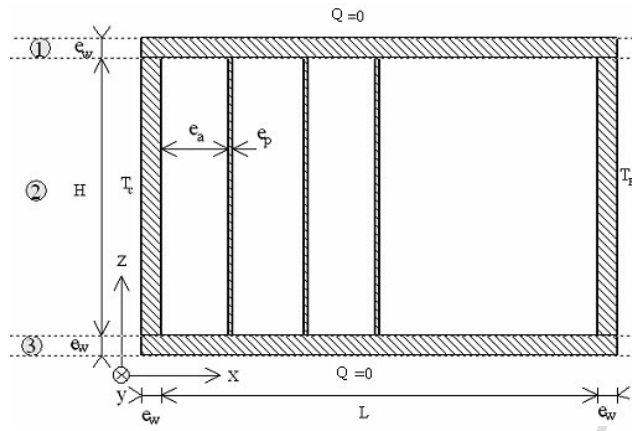


Fig. 1: Studied partitioned enclosure

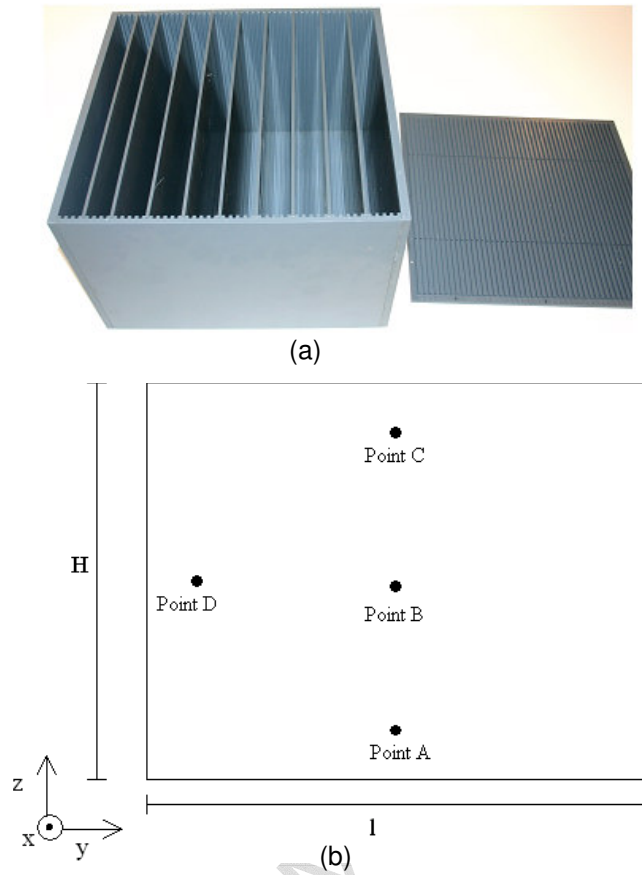


Fig. 2: Experimental enclosure (a) and thermocouples positioning on a partition (b)

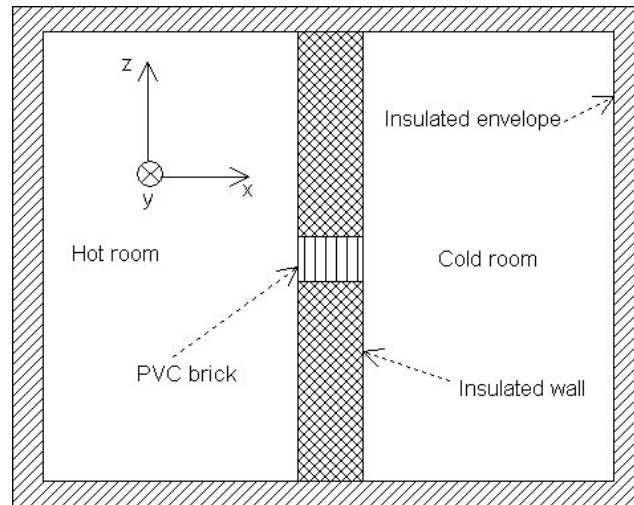


Fig. 3: Climatic chamber

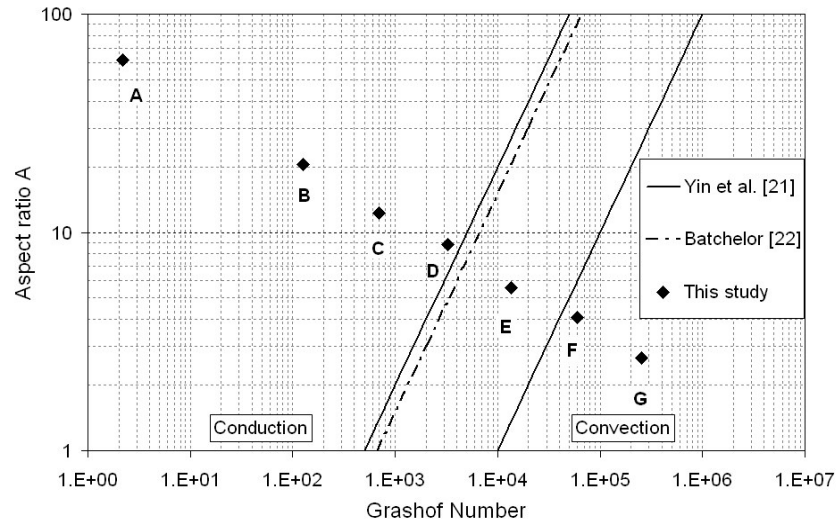


Fig. 4: Conduction - convection limits in an air-filled rectangular enclosure

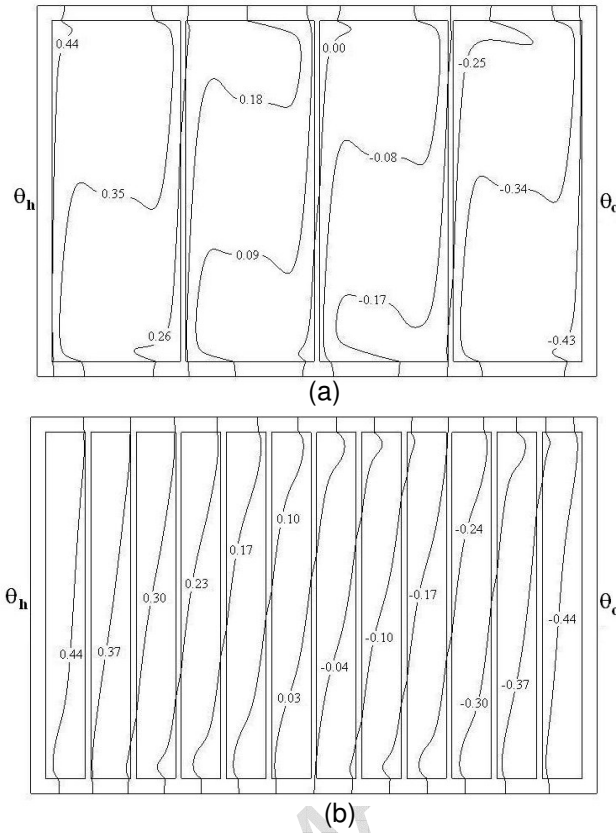


Fig. 5: Dimensionless numerical isotherms in the enclosure G ($N=3$, $T_h-T_c=23.2$ K) (a) and in the enclosure D ($N=11$, $T_h-T_c=29.7$ K) (b)

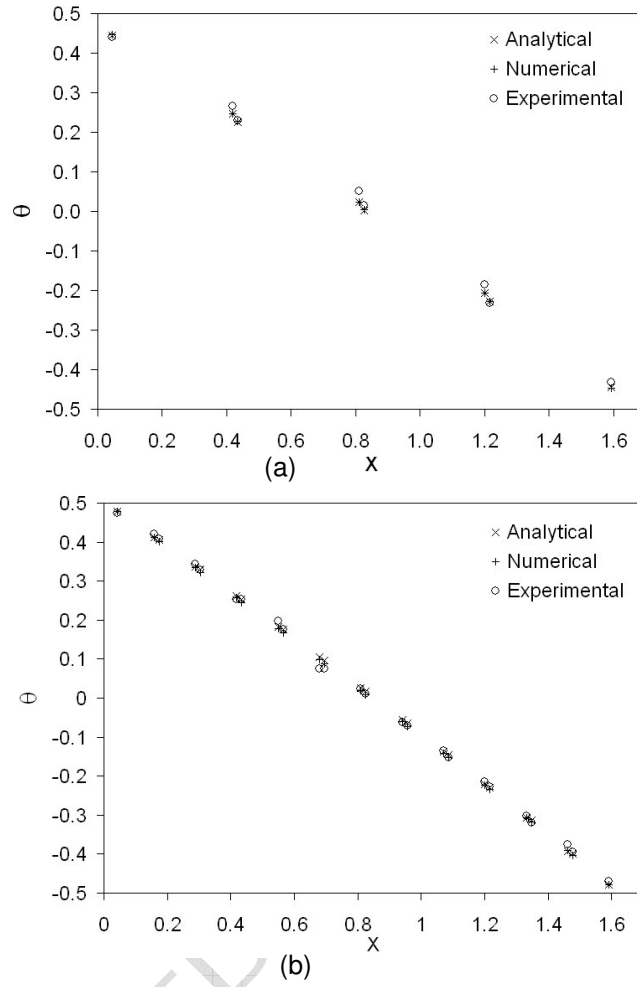


Fig. 6: Analytical, numerical and experimental mean dimensionless temperatures in the enclosure G ($N=3$, $T_h-T_c=23.2$ K) (a) and in the enclosure D ($N=11$, $T_h-T_c=29.7$ K) (b)

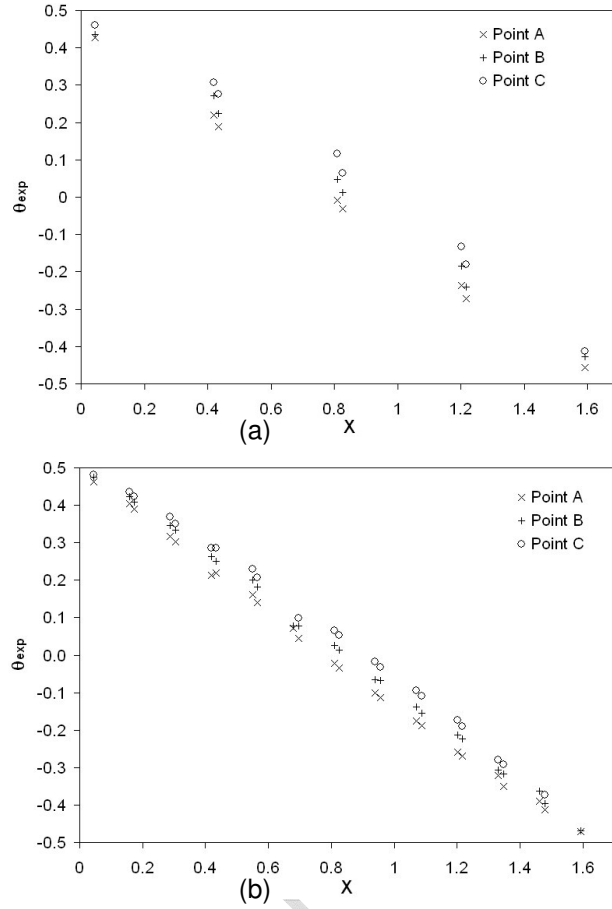


Fig. 7: Evidence of stratification through dimensionless experimental temperatures in enclosure G ($N=3$, $T_h-T_c=23.2$ K) (a) and in enclosure D ($N=11$, $T_h-T_c=29.7$ K) (b)

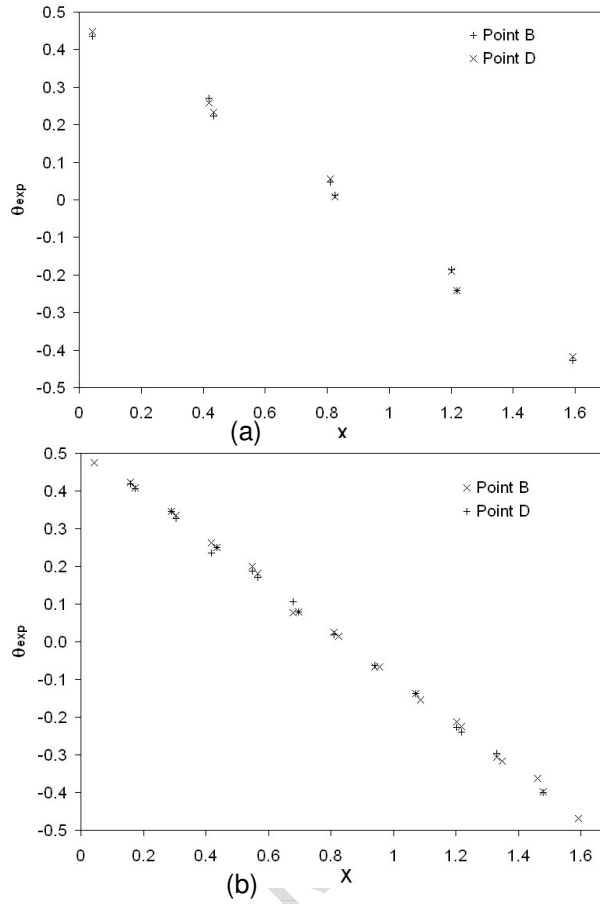


Fig. 8: Evidence of non 3-dimensionnal heat transfer with dimensionless experimental temperatures in the enclosure G ($N=3$, $T_h-T_c=23.2$ K) (a) and in the enclosure D ($N=11$, $T_h-T_c=29.7$ K) (b)

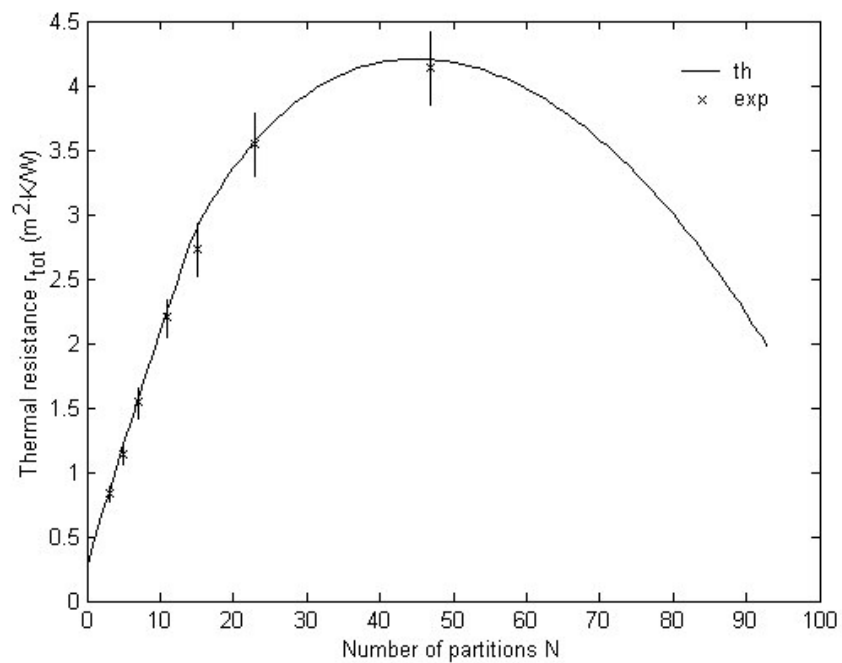


Fig. 9: Thermal resistance r_{tot} versus partitions number N

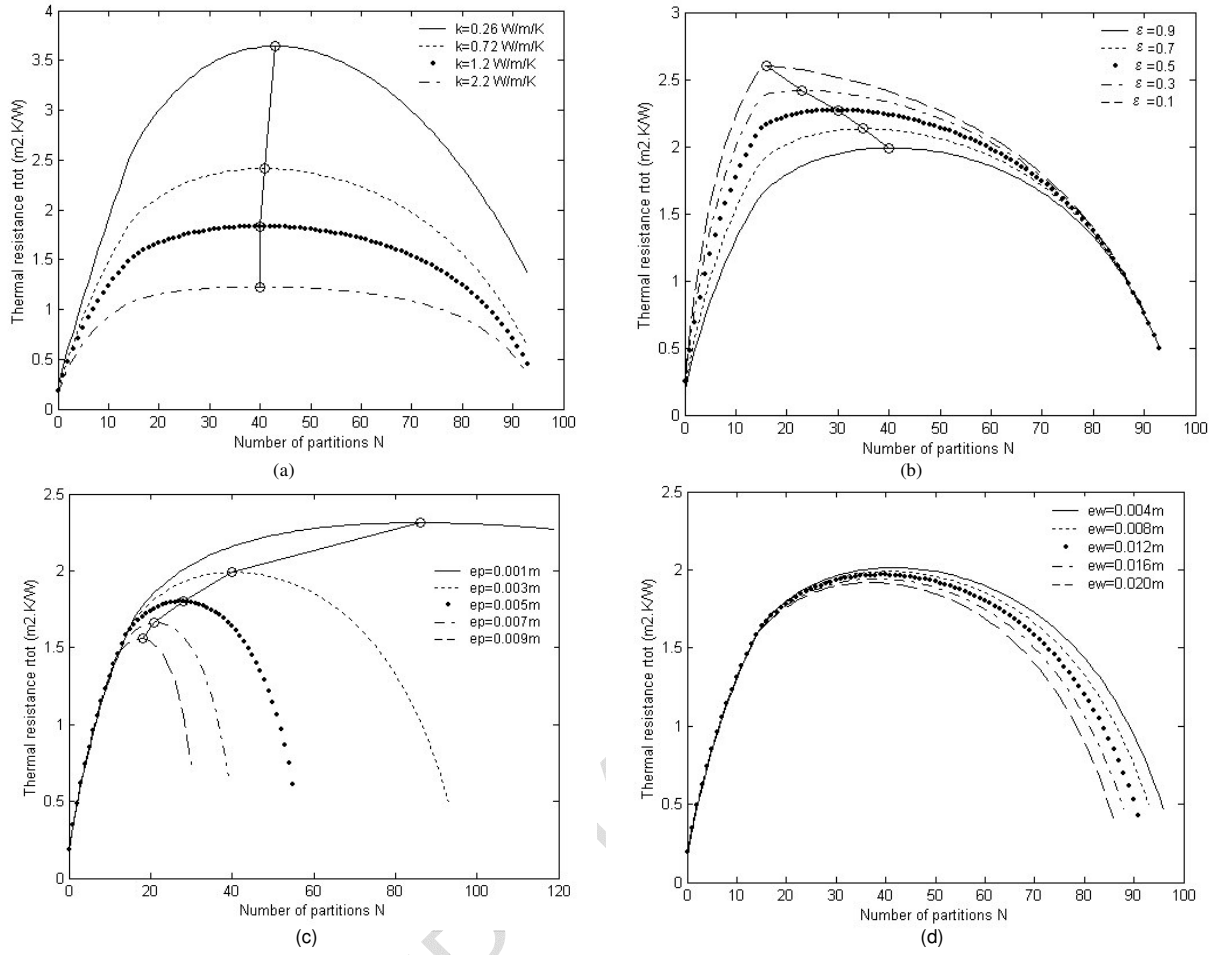


Fig. 10: Thermal resistance r_{tot} vs partitions number N for several materials (a), for several walls emissivities (b), for several partitions thicknesses (c) and for several external vertical walls thickness (d)

Figures caption

Fig. 1: Studied partitioned enclosure

Fig. 2: Experimental enclosure (a) and thermocouples positioning on a partition (b)

Fig. 3: Climatic chamber

Fig. 4: Conduction - convection limits in an air-filled rectangular enclosure

Fig. 5: Dimensionless numerical isotherms in the enclosure G (a) and in the enclosure D (b)

Fig. 6: Analytical, numerical and experimental mean dimensionless temperatures in the enclosure G (a) and in the enclosure D (b)

Fig. 7: Evidence of stratification through dimensionless experimental temperatures in enclosure G (a) and in enclosure D (b)

Fig. 8: Evidence of non 3-dimensionnal heat transfer with dimensionless experimental temperatures in the enclosure G (a) and in the enclosure (b)

Fig. 9: Thermal resistance r_{tot} versus partitions number N

Fig. 10: Thermal resistance r_{tot} vs partitions number N for several materials (a), for several walls emissivities (b), for several partitions thicknesses (c) and for several external vertical walls thickness (d)

Tables

Table 1: Comparison of Nusselt numbers for a differentially heated square cavity ($Ra=10^6$)

		De Vahl Davis [21]	Le Breton et al. [21]	A. Abdelbaki and Z. Zrikem [21]	H. Wang et al. [20]	This study
$\varepsilon=0$	Nu_{cv}	9.270	8.794	9.446	8.852	8.947
$\varepsilon=0.2$	Nu_{cv}	N/A	N/A	N/A	2.337	2.338
	Nu_{rad}	N/A	N/A	N/A	8.399	8.458
$\varepsilon=0.8$	Nu_{cv}	N/A	N/A	N/A	7.873	7.941
	Nu_{rad}	N/A	N/A	N/A	11.208	11.229

Table 2: Configurations of the partitioned enclosure

Name	A	B	C	D	E	F	G
N	47	23	15	11	7	5	3
A	61.3	20.4	12.3	8.8	5.6	4.1	2.7
T_h-T_c	30.2	29.4	23.2	29.7	21.4	28.8	23.2

Table 3: Analytical Nusselt numbers for the enclosure G ($N=3, T_h-T_c=23.2$ K)

Alveolus	1	2	3	4
Nu_{rad}	11.5	10.9	10.3	9.7
Nu_{cv}	5.8	5.9	6.0	6.0

Table 4: Analytical Nusselt number for the enclosure D ($N=11, T_h-T_c=29.7$ K)

Alveolus	1	2	3	4	5	6	7	8	9	10	11	12
Nu_{rad}	4.2	4.1	4.0	3.9	3.8	3.7	3.7	3.6	3.5	3.4	3.3	3.2
Nu_{cv}	1.4	1.4	1.4	1.5	1.5	1.5	1.5	1.5	1.5	1.5	1.5	1.5

Table 5: Numerical Nusselt numbers for the enclosure G ($N=3$, $T_h-T_c=23.2$ K)

Alveolus	1	2	3	4
Nu_{rad}	11.4	10.8	10.2	9.7
Nu_{cv}	4.7	4.9	5.0	4.8

Table 6: Numerical Nusselt numbers for the enclosure D ($N=11$, $T_h-T_c=29.7$ K)

Alveolus	1	2	3	4	5	6	7	8	9	10	11	12
Nu_{rad}	4.2	4.1	4.0	3.9	3.9	3.7	3.7	3.6	3.5	3.4	3.3	3.2
Nu_{cv}	1.2	1.3	1.4	1.4	1.5	1.5	1.5	1.5	1.5	1.5	1.4	1.3